Accumulation of Mutational Load at the Edges of a Species Range

Yvonne Willi,*[,1,2] Marco Fracassetti,[1,2] Stefan Zoller,[3] and Josh Van Buskirk[4]

[1]Institute of Biology, University of Neuchâtel, Neuchâtel, Switzerland

[2]Department of Environmental Sciences, University of Basel, Basel, Switzerland

[3]Genetic Diversity Centre, ETH Zürich, Zürich, Switzerland

[4]Institute of Evolutionary Biology and Environmental Studies, University of Zürich, Zürich, Switzerland

***Corresponding author:** E-mail: yvonne.willi@unibas.ch.

Associate editor: Brandon Gaut

Sequence data used in this study are stored at the European Nucleotide Archive (http://www.ebi.ac.uk/ena) with the accession number PRJEB19338.

Abstract

Why species have geographically restricted distributions is an unresolved question in ecology and evolutionary biology. Here, we test a new explanation that mutation accumulation due to small population size or a history of range expansion can contribute to restricting distributions by reducing population growth rate at the edge. We examined genomic diversity and mutational load across the entire geographic range of the North American plant *Arabidopsis lyrata*, including old, isolated populations predominantly at the southern edge and regions of postglacial range expansion at the northern and southern edges. Genomic diversity in intergenic regions declined toward distribution edges and signatures of mutational load in exon regions increased. Genomic signatures of mutational load were highly linked to phenotypically expressed load, measured as reduced performance of individual plants and lower estimated rate of population growth. The geographic pattern of load and the connection between load and population growth demonstrate that mutation accumulation reduces fitness at the edge and helps restrict species' distributions.

Key words: **distribution limits, genetic drift, genetic load, geographic expansion, leading edge, mutation accumulation, range limits, trailing edge.**

Introduction

A major open question in ecology and evolution is why species have geographically restricted distributions even in the absence of dispersal limitation. One hypothesis is that distribution limits reflect niche limits: Species occur only where environmental conditions allow population persistence (Hutchinson 1957). The evolutionary perspective on this hypothesis is that limits to niche adaptation block range expansion. These limits may include the genetic architecture of niche-relevant traits or constraints created by too much or too little gene flow (Bridle and Vines 2007; Kawecki 2008; Sexton et al. 2009). Here, we argue that mutational load may be an overlooked and important piece in the puzzle of distribution limits. The idea is that mutational load accumulates most readily at distribution boundaries because the demographic history of range edge populations accentuates the importance of genetic drift, which in turn causes decreased fitness near the range edge.

Small populations are prone to genetic drift—the change in allele frequencies due to chance (Wright 1931; Kimura 1955). In addition to reducing genetic variation in the population, drift opposes the effect of purifying selection against deleterious mutations (Wright 1931; Kimura 1957). Consequently, the frequency of deleterious mutations increases and the fitness of individuals is eroded by genetic load, such that small populations can become even smaller (Lande 1988; Lynch et al. 1995). Ecological conditions near the boundaries of species' geographic distributions are conducive to accumulation of genetic load. Habitat suitability often declines from the core of the distribution toward the edge, so that populations at edges are small and isolated (Hengeveld and Haeck 1982; Brown 1984; Sagarin and Gaines 2002). This is supported by evidence that peripheral regions typically harbor reduced genetic variation within populations and higher genetic variation among populations (Eckert et al. 2008). In addition, range margins often include areas of recent expansion produced by serial founder events, as observed in species recovering from the last glaciation cycle (Hewitt 2000; Excoffier et al. 2009). Demographic founder events are accompanied by enhanced genetic drift, which increases the frequency of recessive deleterious mutations along the expansion route (Peischl and Excoffier 2015). In humans, this is illustrated by reduced genetic variation and elevated mutational load, mainly due to higher homozygosity for deleterious alleles, along the historic expansion route out of Africa to Asia and the Americas (Henn et al. 2016). Both scenarios of range edge dynamics—scarcity of good-quality habitat and recent serial expansion—predict that edge populations bear genomic signatures of increased mutational

load with the consequence of reduced rate of population growth rate, which may help maintain distribution boundaries.

Recent simulations show that mutational load is relevant to range boundaries (Henry et al. 2015; Peischl et al. 2015; Gilbert et al. 2017). Henry et al. (2015) studied a 1D array of habitat patches with linearly declining suitability, and observed that the range was restricted by mutational load if migration and population growth rate were small. Peischl et al. (2015) focused on range expansion from a point of origin on a 1D or 2D grid of habitat patches in the absence of an environmental cline and discovered that mutational load could slow or stop the expansion, depending on the presence of recombination. A similar scenario of expansion in the presence of an environmental cline also noted the limiting influence of load, but predicted complex interactions between fitness decline due to load and due to maladaptation (Gilbert et al. 2017). Taken together, these studies suggest that mutational load can, in principle, reduce range expansion and sometimes create a range boundary.

We studied the entire distribution of a plant species, the North American *Arabidopsis lyrata* subsp. *lyrata*, relating the demographic history of populations with their mutational load estimated from genomic and phenotypic data. The current geographic distribution of this species suggests that it was strongly affected by the last glacial maximum (LGM). *Arabidopsis lyrata* occurs from North Carolina and Missouri in the south to the Great Lakes region in the north, with about half of the distribution area having been covered by ice during the LGM. The species is predominantly outcrossing, but there are selfing populations (Foxe et al. 2010) and they tend to be located at the edge of the range (Griffin and Willi 2014). The most comprehensive phylogeographic study performed so far showed that *A. lyrata* consists of two ancestral lineages, one in the east in the Appalachians and another in the Midwest, with the border between lineages running through Lake Erie (Griffin and Willi 2014). Earlier studies had already suggested clustering in the east and west (Foxe et al. 2010; Willi and Määttänen 2010). Griffin and Willi (2014) also found a decline in genetic diversity toward the margins of the two subranges, indicating a demographic history of small population size at the edge, along with evidence of long-term isolation in the south and recent range expansion in the northwest.

This study addressed the following questions: 1) What is the history of southern populations and the precise geography of northern range expansion? 2) Does the decline in within-population genetic diversity coincide with the geographical context of recolonization after the last glacial maximum and with long-term isolation of older populations? 3) Does the signature of mutational load increase with distance along the recolonization route and with distance of older populations to the cores from which recolonization began? 4) Are genomic estimates of mutational load correlated with phenotypic estimates of load and projected population growth rate? And 5), what is the magnitude of fitness decline over the observed range of mutational load? Because our study included eight predominantly selfing populations and two with a mixed-mating system, we also tested whether genetic diversity and mutational load vary with the mating system.

Results

Population Relatedness and Demographic History

The starting point of our analysis was to obtain a relatedness tree for 52 populations of *A. lyrata* based on sequence data, to reveal the geography of postglacial range expansion and the history of southern populations. We resequenced the entire nuclear genome in pools of 25 individuals per population at an average sequencing depth of 128×. The depth of sequencing allowed us to detect SNP frequencies close to 2%, which is the lowest possible frequency occurring in a sample of 25 individuals per population. The range-wide history of North American *A. lyrata* was revealed by establishing a relatedness tree that allowed for the occurrence of past admixture events, using >120,000 single nucleotide polymorphisms (SNPs) at sites sequenced in all populations (supplementary fig. S1*A*, Supplementary Material online). The new relatedness tree confirmed the division between eastern and western clades and detected admixture in the Lake Erie region (supplementary fig. S1, Supplementary Material online). Furthermore, it suggested that postglacial recolonization occurred ~20,000 years ago, originating from Pennsylvania in the east and from Wisconsin in the western clade (supplementary fig. S1*A*, Supplementary Material online). We projected the relatedness tree onto the map, and defined the core area as the geographic location of the most recent common ancestor of all sampled populations that are in an area known to have been covered by ice (supplementary fig. S1*B*, Supplementary Material online). From the two core areas, indicated by triangles in figure 1*A*, recolonization extended mainly along the Appalachians toward both north and south in the eastern clade, and north to Lake Superior and later eastward to Lake Huron and Lake Erie in the western clade. Rear-edge populations within unglaciated areas arose from divergences older than the core and were located in coastal New Jersey in the east and in Missouri and Iowa in the west. Thus, the southern border of *A. lyrata* had both kinds of edges: a leading edge with recently colonizing populations in the south-east and a typical rear edge with old, isolated populations in the southwest.

We inferred the history of genetic drift in *A. lyrata* using two measures of within-population genomic diversity in intergenic regions (defined as >1000 base pairs from the nearest gene; Ross-Ibarra et al. 2008). Watterson's θ is the number of polymorphic sites adjusted for the length of sequences and for the number of haploid samples (Watterson 1975), and Tajima's π is a measure of heterozygosity calculated as the mean proportion of pairwise differences between any two sequences (Tajima 1983). Both measures of genomic diversity declined with increasing distance from the core area in both clusters (table 1 and figs. 1*A* and 2*A* and supplementary figs. S2*A* and S3*A* and *B*, Supplementary Material online). Distances were the sum of

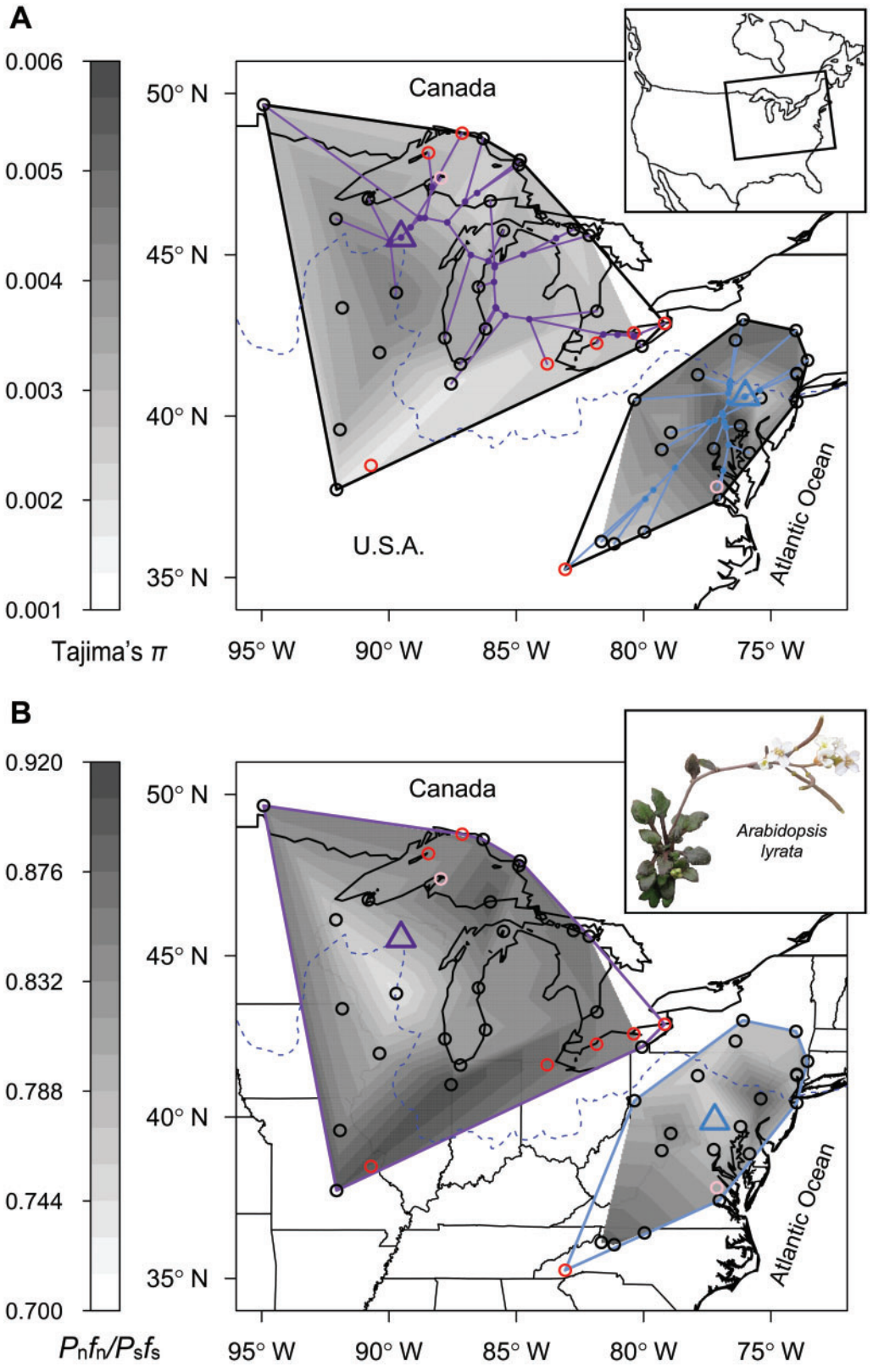

Fig. 1. Geographic pattern of the genomic signatures of mutational load in North American *Arabidopsis lyrata*. (*A*) Tajima's π estimated from SNPs in intergenic regions. (*B*) Ratio of nonsynonymous to synonymous polymorphic sites in coding DNA sequences adjusted for the frequencies of the derived allele ($P_n f_n / P_s f_s$). Darker gray indicates higher levels of diversity (*A*) and load (*B*); both surfaces were estimated based on outcrossing populations only. Minimum convex polygon hulls surrounding populations of the western and eastern ancestral genetic clusters are drawn in black (*A*) or purple and blue (*B*). Triangles indicate the core areas from which recolonization began after the most recent glacial maximum. In panel (*A*), lines from these cores are recolonization routes revealed by projecting the population phylogeny on the map, with small circles representing nodes in the phylogeny. Open circles are the populations sampled in this study: outcrossing

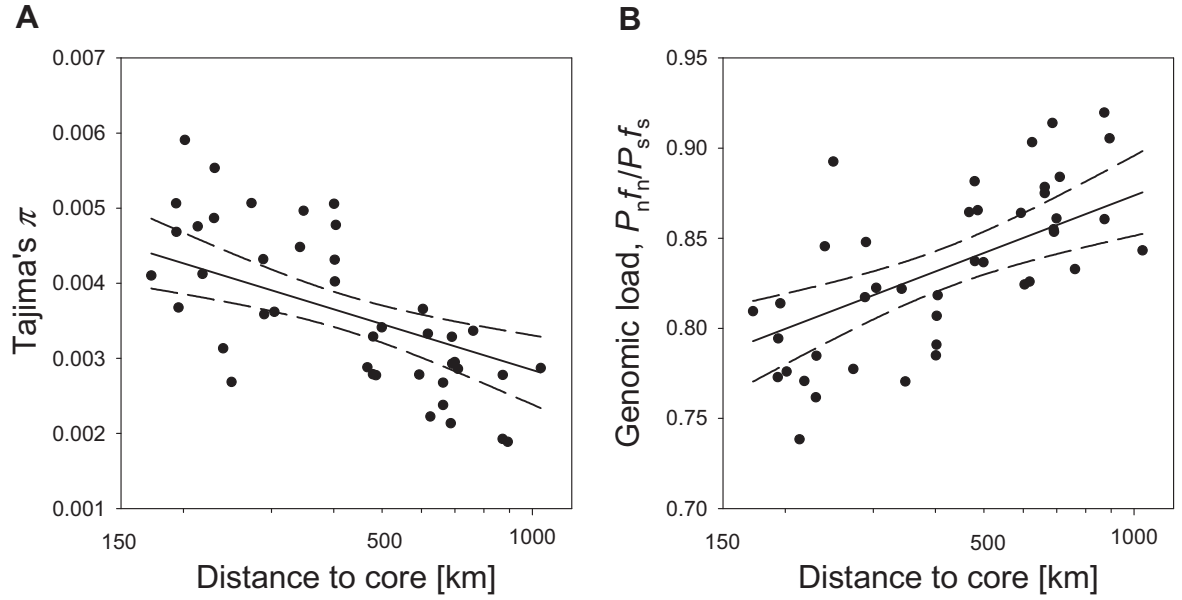

Fig. 2. Correlations between genomic diversity, a genomic estimate of mutational load, and the distance from the core of the distribution in North American *Arabidopsis lyrata*. (*A*) Tajima's π estimated from SNPs in intergenic regions. (*B*) Ratio of nonsynonymous to synonymous polymorphic sites in coding DNA sequences adjusted for the frequencies of the derived allele ($P_n f_n / P_s f_s$). Lines depict the model-predicted regression (solid line) and 95% confidence interval (dashed lines) based on 42 outcrossing populations (black symbols). Values were first corrected for ancestral cluster. Coefficients and variance explained are reported in table 1.

great circle distances along the map-projected nodes back to the core location (for populations descended from the core population) or the great circle distance directly to the core (for populations originated from older splits). Populations at both the leading and rear edges showed increasing signals of small population size with distance from the core ($N = 37$ outcrossing populations along expansion routes to leading edges with diversity estimates corrected for cluster, Pearson correlation between θ and [$\log_{10}$-transformed] distance: $r = -0.53$, π and distance: $r = -0.54$; $N = 4$ outcrossing populations of the western rear edge, θ and distance: $r = -0.78$, π and distance: $r = -0.82$). We also found that selfing populations had lower genomic diversity than outcrossing populations (table 1 and supplementary fig. S4*A* and *B*, Supplementary Material online), in line with theory predicting that self-fertilization reduces the effective population size relative to random outcrossing (Pollak 1987).

Populations far from the core showed a genomic signature of recent population decline. There was a significant increase in Tajima's D—θ subtracted from π for intergenic regions, scaled to its SD (Tajima 1989)—with ($\log_{10}$-transformed) distance from core (linear coefficient = 0.37, $P = 0.0397$). When sequences are not influenced by selection, positive values of Tajima's D indicate recent population decline.

Genomic Estimates of Mutational Load

Whereas genomic diversity declined from core to edge, genomic estimates of mutational load increased toward the edge in both ancestral clusters (figs. 1*B* and 2*B*). Table 1 presents results for three measures of load calculated for each population using coding DNA sequences (CDS). The proportion of nonsynonymous polymorphic sites, $P_n/(P_n+P_s)$, is an estimate of the efficacy of purifying selection with higher values indicating less purifying selection (Lohmueller et al. 2008; Stoletzki and Eyre-Walker 2011). The ratio of the number of nonsynonymous to synonymous polymorphic SNPs multiplied by the ratio of frequencies of the alleles that are derived relative to *A. thaliana*, $P_n f_n / P_s f_s$, depicts changes in the site frequency spectrum of presumably deleterious alleles relative to the spectrum of presumably neutral alleles (Peischl and Excoffier 2015). An increase of $P_n f_n / P_s f_s$ reflects higher load and is expected under increasing genetic drift. Finally, the sum of squared frequencies of derived polymorphic SNPs with presumably high phenotypic impact relative to the sum of low-impact SNPs, $\sum f^2_{high} / \sum f^2_{low}$, also depicts relative changes in the site frequency spectra, but focuses on a different class of potentially deleterious SNPs than does $P_n f_n / P_s f_s$. High-impact SNPs included those likely to damage the gene product by causing gain or loss of a start codon, stop codon, or splice site (Cingolani et al. 2012). Furthermore, $\sum f^2_{high} / \sum f^2_{low}$ assumes that deleterious mutations are fully recessive and expressed

Fig. 1. Continued
(black), mixed-mating (pink), and selfing (red). Unshaded areas within the polygon hulls are regions with no outcrossing populations. The dashed blue line indicates the maximum extent of the ice sheet during the last glacial maximum. Genomic diversity declined and mutational load climbed with increasing distance from the core areas.

Table 1. Linear Models Testing for Relationships between Population Genomic Parameters and Genetic Cluster (east, west), Distance from the Core Area ($\log_{10}$-transformed; see fig. 1A), and Mating System (outcrossing O, selfing/mixed-mating S) (A) and a Reduced Model with Outcrossing Populations Only (B).

Source	df_{num}	Measures of Genomic Variation				Measures of Mutational Load					
		Watterson's θ		Tajima's π		$P_n/(P_n+P_s)$		P_nf_n/P_sf_s		$\sum f^2_{high}/\sum f^2_{low}$	
		Coeff.	*P*	Coeff.	*P*	Coeff.	*P*	Coeff.	*P*	Coeff.	*P*
A. All Populations											
Ancestral cluster (east)	1	5.5E-4	0.0607	6.8E-4	0.0045	2.8E-3	0.1763	−7.6E-3	0.5715	7.0E-4	0.4146
Distance to core	1	−2.8E-3	<0.0001	−2.3E-3	<0.0001	1.7E-2	0.0004	1.1E-1	0.0002	5.1E-3	0.0070
Mating system (O)	1	1.7E-3	<0.0001	1.7E-3	<0.0001	−1.4E-2	<0.0001	−1.1E-1	<0.0001	−6.9E-3	<0.0001
R^2			0.66		0.74		0.58		0.68		0.61
B. Outcrossing Populations											
Ancestral cluster (east)	1	3.1E-4	0.3622	4.5E-4	0.0860	3.4E-3	0.0276	5.1E-3	0.6763	1.5E-3	0.0267
Distance to core	1	−3.5E-3	<0.0001	−2.8E-3	<0.0001	1.8E-2	<0.0001	1.5E-1	<0.0001	6.8E-3	<0.0001
R^2			0.49		0.56		0.44		0.49		0.36

NOTE.—Dependent variables were Watterson's θ and Tajima's π estimated for intergenic regions, and three measures of mutational load estimated for coding DNA sequences: the proportion of nonsynonymous polymorphic sites [$P_n/(P_n+P_s)$], the ratio of nonsynonymous to synonymous polymorphic sites adjusted for the frequencies of the derived allele (P_nf_n/P_sf_s), and the sum of squared allele frequencies of derived SNP variants with a high phenotypic impact relative to the sum of squared frequencies of derived, segregating SNPs with a low phenotypic impact ($\sum f^2_{high}/\sum f^2_{low}$). Sample sizes in A were 52 resequenced North American *Arabidopsis lyrata* populations and in B were 42 outcrossing populations. Linear coefficients (coeff.) are reported.

only when homozygous. P_nf_n/P_sf_s and $\sum f^2_{high}/\sum f^2_{low}$ should be more accurate because they account for the frequency of the deleterious variant and therefore its probability of occurring in the homozygous state (Simons et al. 2014; Peischl and Excoffier 2015). The geographic pattern was qualitatively the same for the three measures: load increased with distance from the core (figs. 1*B* and 2*B* and supplementary figs. S2*B* and *C* and S3*C*–*E*, Supplementary Material online). Populations at both the leading and rear edges showed positive correlations between mutational load and distance from core [$N = 37$ outcrossing populations along expansion routes to leading edges with load estimates corrected for cluster, Pearson correlation between $P_n/(P_n+P_s)$ and ($\log_{10}$-transformed) distance: $r = 0.50$; P_nf_n/P_sf_s and distance: $r = 0.55$; $\sum f^2_{high}/\sum f^2_{low}$ and distance: $r = 0.48$; $N = 4$ outcrossing populations of the western rear edge, $P_n/(P_n+P_s)$ and distance: $r = 0.99$; P_nf_n/P_sf_s and distance: $r = 0.89$; $\sum f^2_{high}/\sum f^2_{low}$ and distance: $r = 0.83$]. Mutational load was also higher in selfing populations (supplementary fig. S4*C*–*E*, Supplementary Material online). All measures of load were highly correlated with the two estimates of genomic diversity (supplementary fig. S5, Supplementary Material online).

Two analysis evaluated whether positive selection has increased the frequency of derived nonsynonymous SNPs in edge populations. First, we tested whether indicators of positive selection and mutational load were positively associated. None of the three estimates of mutational load [$P_n/(P_n+P_s)$, P_nf_n/P_sf_s, or $\sum f^2_{high}/\sum f^2_{low}$] was positively correlated with the fraction of 5000-bp windows from coding regions having a signature of positive selection according to the combined *DH* test of Zeng et al. (2006) (outcrossing populations: $N = 42$, $r = 0.26/-0.05/-0.02$, all $P > 0.1$; selfing populations: $N = 10$, $r = -0.13/-0.03/-0.03$, all $P > 0.7$). The second analysis classified nonsynonymous SNPs according to whether they are likely to be tolerated or deleterious to protein function, using the SIFT 4 G algorithm (Vaser et al. 2016). The ratio of deleterious to tolerated nonsynonymous SNPs, weighted by the ratio of their mean frequencies, was in all cases positively correlated with the three genomic estimates of mutational load, $P_n/(P_n+P_s)$, P_nf_n/P_sf_s and $\sum f^2_{high}/\sum f^2_{low}$ (outcrossing populations: $N = 42$, $r = 0.33/0.57/0.79$, all $P < 0.05$; selfing populations: $N = 10$, $r = 0.81/0.73/0.82$, all $P < 0.05$). Taken together, these two analyses strongly indicate that genomic estimates of mutational load do not result from positive selection and do reflect negative impacts on protein function.

Phenotypic Estimates of Mutational Load

A common garden experiment verified that genomic estimates of mutational load were linked with both a phenotypic estimate of load and the projected rate of population growth. We measured heterosis, which reflects load to the extent that it is caused by recessive deleterious mutations, by comparing the performance of progeny from artificial crosses between plants from the same and a different population (Willi 2013). Performance was measured as germination probability multiplied by the sum of flowers produced by the plant over the first three growing seasons in an outdoor garden. Heterosis was positively correlated with all three measures of genomic load; the strongest relationship was with P_nf_n/P_sf_s, the frequency-adjusted ratio of nonsynonymous to synonymous polymorphic sites ($N = 18$ populations, $r_S = 0.66$, $P = 0.0032$; fig. 3*A* and supplementary table S1, Supplementary Material online). Population growth rate (λ), calculated from life tables parameterized using data from plants produced by within-population crosses and followed for 8 years in the common garden, was negatively correlated with genomic estimates of load (for P_nf_n/P_sf_s: $N = 18$ populations, $r_s = -0.75$, $P = 0.0003$; fig. 3*B* and supplementary table S1, Supplementary Material online). The predicted decline in population growth rate caused by mutational load was up to 53% in outcrossing populations and 94% in selfing

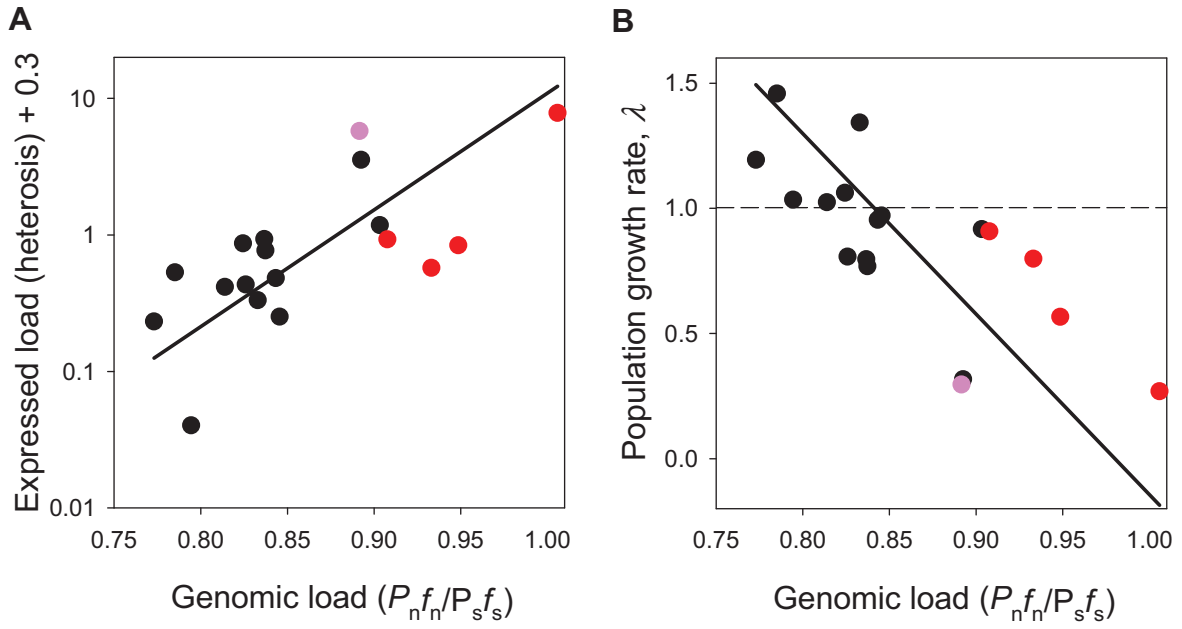

Fig. 3. Correlations between a phenotypic measure of load, population growth rate, and a genomic estimate of mutational load in North American *Arabidopsis lyrata*. (*A*) Heterosis is the difference in flower production between offspring of between- and within-population crosses. (*B*) Population growth rate (λ) was estimated from life tables for each population over 8 years in the outdoor garden. The genomic estimate of load is the ratio of nonsynonymous to synonymous polymorphic sites in coding DNA sequences adjusted for the frequencies of the derived allele ($P_n f_n/P_s f_s$). Lines depict major axis regressions based on 13 outcrossing (black symbols), 1 mixed-mating (pink), and 4 selfing populations (red).

populations. Population growth rate for plants produced by between-population crosses also declined with genomic estimates of load, but with a less negative slope (supplementary table S1, Supplementary Material online). This suggests that deleterious mutations have some effect on phenotypic performance when heterozygous (i.e., are only partially recessive).

Discussion

There are distinct ecological and evolutionary viewpoints on the causes of geographic range limits. Ecological processes include dispersal limitation and harsh environmental conditions that reduce population growth (Kawecki 2008; Sexton et al. 2009). In our system, dispersal limitation is unlikely because ecological niche modelling demonstrates that northern and southern distribution limits coincide with the limits of suitable habitat (Lee-Yaw et al. 2017). Lee-Yaw et al. also discovered that habitat suitability generally declines with geographic distance from the center of the range and that the distance to the environmental niche center increases with peripherality in all directions except toward the east. Important niche-determining environmental variables were observed to change in a linear or step-like function near range edges. The evolutionary perspective on range limits is that populations are unable to extend into more marginal habitat because adaptation is constrained by gene flow or too little genetic variation in ecologically relevant traits (Bridle and Vines 2007; Kawecki 2008; Sexton et al. 2009). This study highlights a new mechanism of range limitation that bridges these ecological and evolutionary perspectives by linking genetic drift and mutation accumulation with demography and population growth rate.

The new model states that species distribution limits can emerge due to neutral processes under realistic scenarios involving either stable or expanding distributions. One scenario applies to small and isolated populations occupying patchy and marginal habitat at relatively stable range edges. Adaptation to marginal habitat is constrained because drift erodes genetic variation and mutation accumulation reduces population growth rate such that populations cannot compensate for selective deaths (Haldane 1957). A second scenario applies to edge populations created by recent range expansion. These populations have experienced severe drift during serial demographic founder events, and this creates a signature of mutational load that can persist for thousands of generations (Peischl and Excoffier 2015). Here again, genetic variation is eroded, mutations accumulate, and adaptation stalls. This model is supported by recent simulation studies showing that mutation accumulation can reduce the rate of a range expansion and in some cases create a range boundary when the environment shows clinal variation in carrying capacity and migration is limited, and if recombination does not occur (Henry et al. 2015; Peischl et al. 2015; Gilbert et al. 2017).

This model of mutation accumulation is likely of general importance in wild species. Many taxa exhibit declining neutral marker diversity toward the edge of the distribution, indicating strong genetic drift (Eckert et al. 2008). Our results show that drift goes hand-in-hand with accumulation of mutational load and reduced population growth rate. We propose that many species with declining genetic diversity at range edges will also exhibit mutational load and reduced individual fitness in edge populations. Based on population growth rates estimated in our study, the maximal decline

predicted to be caused by mutational load is 50% in outcrossing populations and up to 90% for selfing populations. This suggests that ecological studies observing reduced population growth at distribution edges (Gaston 2009) may be documenting at least in part the consequences of increased load rather than a response to marginal habitat. Indeed, eco-evolutionary dynamics involving mutational load could be important whenever small population size or demographic bottlenecks occur, including under abiotic environmental stress or periodic population cycles.

The transition to selfing from ancestral outcrossing has occurred multiple times in North American *A. lyrata*, and most of these mating system shifts have occurred in populations near the edges of the species' distribution (Griffin and Willi 2014). This study shows that estimates of genomic diversity are lower and those of mutational load higher in selfing populations, even after accounting for their biased geographic position near range edges. This contradicts the theoretical expectation that selfing facilitates purging of load by ensuring that deleterious mutations are expressed frequently in the homozygous state and are therefore exposed to purifying selection (Ohta and Cockerham 1974). But our results agree with more recent work by Glémin (2003), who showed that purging under nonrandom mating requires minimal effective population sizes in the thousands if mutations are weakly deleterious. Our findings also support the hypothesis that selfing is an evolutionary dead-end because of mutation accumulation, as predicted by theory (Lynch et al. 1995) and confirmed by experiments showing that *A. lyrata* in selfing populations perform relatively poorly (Willi 2013). This implies that the role of mutational load in maintaining distribution boundaries may be especially strong in *A. lyrata* because the geographic pattern observed in outcrossing populations (e.g., figs. 1*B* and 2*B*) will be accentuated by the location of selfing populations near range limits.

We suspect that genetic load at range edges—independent of mating system—will become increasingly relevant under climate change. Rapid distributional shifts toward higher latitude or elevation will accentuate mutational load and decrease individual fitness in leading-edge populations. It has been suggested that rear-edge populations could serve as a source of adaptive variation as higher latitude populations decline under a warmer climate (Hampe and Petit 2005), but the burden of deleterious mutations carried by these populations because of their long-term isolation and small size could outweigh the advantages of whatever adaptive genetic variation they possess.

Materials and Methods

Sequencing and SNP Detection

Fifty-two populations of *A. lyrata*, spanning the entire North American distribution of the species, were sampled between 2007 and 2014. DNA of 25 field collected individuals per population was extracted, quantified, pooled, and fragmented with the Nextera Kit (Illumina, San Diego, CA) (Fracassetti et al. 2015). Each library was pair-end (PE100) sequenced by an Illumina2000 sequencer with three other libraries per lane, on four replicate lanes. Reads were demultiplexed and the adapters removed. Reads were then trimmed from the 3′ end with a base quality cutoff of 20, using the program PoPoolation (Kofler et al. 2011). We used all scaffolds of the nuclear genome of *A. lyrata* as the reference genome for the initial alignment (Hu et al. 2011), along with the chloroplast and mitochondrial genomes of *Arabidopsis thaliana* (https://www.arabidopsis.org/). Two large sections of scaffold 2 of the *A. lyrata* genome were masked because they had high sequence homology with parts of the *A. thaliana* chloroplast genome (positions: 8746475–8835273 and 9128838–9212301). The reference was indexed and the reads aligned with the BWA-MEM algorithm of the BWA program (Li and Durbin 2009). Duplicates were removed with the MarkDuplicates tool of Picard (http://broadinstitute.github.io/picard). We filtered reads for a minimum mapping quality score of 20 and unambiguously aligned read pairs with the program SAMtools (Li et al. 2009). Based on the final BAM file (data deposited at: European Nucleotide Archive accession number PRJEB19338), one pileup file per population was produced. Sequencing of all populations yielded more than 13 billion mapped paired-end reads. After applying an initial read depth cutoff (25–500×), removing duplicates and filtering for mapping quality, an average of 220 million paired-end reads per populations mapped unambiguously to 67% of the *A. lyrata* nuclear genome.

Pileup files were filtered and split for SNP calling. Further filtering involved setting minimum and maximum depth of sequencing, and removing regions with neighboring indels and regions of interspersed repeats using PoPoolation (Kofler et al. 2011) and RepeatMasker (Smit et al. 2015). Finally, two new pileup files were created for each population, for two types of genomic regions: intergenic regions 1000 bp away from the nearest gene, and coding DNA sequences. SNPs were called with the program VarScan (Koboldt et al. 2009) on the original pileup file and the two reduced ones. SNPs from the original file were used to produce the relatedness tree, whereas those from intergenic regions were used to estimate genomic diversity. We chose the settings for SNP calling to minimize false positives and false negatives while maximizing data availability. Range of coverage was set to 25–500 for the generation of the relatedness tree and 50–500 for intergenic estimates of diversity. Minimum variant allele count was 3, and the minimum frequency of the minor allele was set to 0.03. Finally, the threshold *P* value for Fisher's exact test was 0.15 and the SNPs with extreme strand bias were removed. The pileup file of coding regions (CDS) was used to estimate genomic load. For calculating the proportion of nonsynonymous polymorphic sites to all polymorphic sites, we used a more stringent range of coverage (100–500) so that we could detect a minimum allele frequency of 0.03. For one population (MO3), the range was set to 75–500 because that population had fewer paired end (PE) reads. Other settings for SNP-calling were the same as for intergenic regions. For the two other measures of load described below, settings for SNP detection were liberal and more stringent filtering was applied later. The VarScan output files were then used to

create separate SNP files for each of the scaffolds representing the eight nuclear chromosomes.

Population Relatedness Tree and Demographic History

For the population relatedness tree, there were 127,725 SNPs (of which 32,157 were in intergenic regions) sequenced at sufficient depth for all populations. Based on the SNP frequency data in windows of 500 SNPs, a likelihood-based tree was produced with the program TreeMix (Pickrell and Pritchard 2012) using *A. halleri* as the outgroup (population Ha31 [Fischer et al. 2013]). Seven admixture events were allowed, because a further increase did not change the number of significant admixture events with the four-population test implemented in TreeMix. Fifty trees were produced. We accepted the tree with second highest likelihood because the set of trees with the highest likelihood had topologies that were historically unlikely, with populations from formerly glaciated Lake Erie at the base of the eastern cluster and two bouts of immigration from nearby ON3. Five admixture events were significant: three from Missouri northward to adjacent areas and two from the east to Lake Erie. One event from the east to Missouri could not be tested for significance because no proper pairing of populations was possible. We dated the tree based on the estimated divergence time of 337,400 years between *A. halleri* and European *A. lyrata* (Roux et al. 2011). Time calibration was done with the chronos function of the R package "ape" (Paradis et al. 2004), based on a "correlated" model with a smoothing parameter (λ) of 0 and allowing different mutation rates in ten different branch categories. The geographic layout of the population phylogeny was plotted on the map with bivariate location information of ancestral nodes revealed by maximum likelihood (Sidlauskas 2008; Revell 2012).

Core areas were defined as the geographic location of the most recent common ancestor of all sampled populations that are in an area known to have been covered by ice. Populations were considered "rear-edge" when they arose from divergences older than the cores. For every population, distance from the respective core was calculated, either as the sum of great circle distances along the map-projected nodes back to the core location (for populations descended from the core population) or as the great circle distance directly to the core (for rear-edge populations).

We inferred demographic history using within-population genomic diversity, that is, Watterson's θ (Watterson estimator), Tajima's π (Tajima's estimator), and Tajima's D within intergenic regions. All three parameters were estimated for windows of 5000 bp on the reference *A. lyrata* genome with the program NPStat (Ferretti et al. 2013) based on VarScan SNP lists. We set the minimum allele count at 3 ($m > 2$ in NPStat). For each population and parameter, the median weighted by the number of sites with sequence information was taken across all 5000-bp windows to give summary measures of genetic diversity (Watterson's θ and Tajima's π, supplementary table S2, Supplementary Material online) and the difference between π and θ, Tajima's D.

Estimates of Load

There were three genomic measures of load calculated for coding DNA sequences (CDS) (supplementary table S2, Supplementary Material online). One was $P_n/(P_n+P_s)$, the fraction of nonsynonymous polymorphic sites to all polymorphic sites. Simulations have shown that $P_n/(P_n+P_s)$ generally increases under a bottleneck because purifying selection is less effective (Lohmueller et al. 2008). The number of polymorphic sites was calculated with NPStat, based on the outgroup of *A. thaliana* and annotation information from *A. lyrata*. The second measure was based on the ratio of polymorphic nonsynonymous to synonymous SNPs, but was adjusted for variation among populations in the frequency spectra by multiplying P_n/P_s by the ratio of mean frequency of nonsynonymous derived SNPs to mean frequency of synonymous derived SNPs, f_n/f_s. Reference for determining which SNP was derived was the *A. thaliana* genome. The resulting quotient, which we call $P_n f_n/P_s f_s$, is based on the expectation that populations at range edges have altered frequency distributions, with generally fewer segregating sites but proportionally more high-frequency variants, many of which have deleterious effect (Peischl and Excoffier 2015). Counts and frequencies for the two types of SNPs were extracted with the program SnpEff (Cingolani et al. 2012). In supplementary figure S6, Supplementary Material online, we show allele frequency spectra for nonsynonymous SNPs from three examples each of central outcrossing populations, range-edge outcrossing populations, and range-edge selfing populations. The third measure of load accounted for the phenotypic impact of mutations: $\sum f^2_{high} / \sum f^2_{low}$ was the ratio of the sum of squared (derived) frequencies of segregating nonsynonymous SNPs of high impact to low impact. We assessed the likely phenotypic impact for each SNP with the program SnpEff (Cingolani et al. 2012). Input files for SnpEff were SNP lists from coding regions for each population (scripts to prepare input files on: https://github.com/fraca/PWGS2) and a customized SnpEff database. For these analysis, an *A. thaliana* outgroup reference with *A. lyrata* position information was used from a multiple genome alignment of the reference genomes of *A. thaliana* TAIR 10 and *A. lyrata* version 1 (Dubchak et al. 2009) (http://pipeline.lbl.gov/downloads.shtml), and annotation information from *A. lyrata* (Rawat et al. 2015). *Arabidopsis lyrata* regions without alignment were encoded as missing values.

We tested the potential confounding impact of positive selection on the accumulation of high-frequency SNPs with the combined *DH* test (eqn 15 in Zeng et al. 2006). Observed values of Tajima's *D* and Fay and Wu's *H* were calculated for 5000-bp windows of the *A. lyrata* reference genome and sequences of CDS regions with the program NPStat (Ferretti et al. 2013). We used the program ms (Hudson 2002) to determine the distributions of Tajima's *D* and Fay and Wu's *H* under a neutral model by simulating genotypes 25,000 times with fixed numbers of segregating sites matching the range observed in our data set (i.e., between a minimum set to 5, and 450). We then used the bisection algorithm (Press et al. 1992) to derive critical values of the joint significance of *D* and *H* for a one-sided test with $\alpha = 0.05$, which we

applied to the observed values for each 5000-bp window. The fraction of windows with a significant signature of positive selection was ln-transformed and correlated with genomic estimates of mutational load both for outcrossing and selfing populations.

Whether nonsynonymous polymorphic SNPs were deleterious or tolerated was estimated by the SIFT 4 G program and the protein sequences of *A. lyrata* provided by SIFT 4 G (Vaser et al. 2016). Input SNP lists were VarScan files with reference information from *A. lyrata*. SIFT 4 G output files were assembled to one file, and merged with the SnpEff output. For each population, the ratio of deleterious SNPs to tolerated SNPs was multiplied by the ratio of their mean frequencies and correlated with genomic estimates of mutational load.

Phenotypically based estimates of load were available from a common garden experiment including 18 *A. lyrata* populations (Willi 2013). We equated load with the heterosis effect of between- versus within-population crosses. In theory, heterosis detected in a common environment is either due to dominance (recessive deleterious mutations have no or reduced fitness effect when heterozygous) or overdominance (heterozygote advantage) (Charlesworth and Willis 2009). Heterosis therefore reflects load only to the extent that it is caused by recessive deleterious mutations. Seeds for the crossing experiment were collected in the field from about 30 plants per population. One offspring per seed family was raised, and twelve per population were randomly selected as being pollen recipients in crosses. These twelve were crossed with a haphazardly chosen plant from the same population and a haphazardly chosen plant from another, randomly chosen population. Two offspring per cross were raised in tubs placed in an outdoor garden. We monitored plant performance for three vegetative periods. The experiment started with 876 tubs with (mostly) four seeds. After a short germination period in a glasshouse, one seedling per tub was randomly selected and kept, and tubs were moved to a garden in Zürich, Switzerland. There were two spatial blocks, with one tub per cross in each block. Performance was measured as the rate of germination in a tub multiplied by the sum of flowers produced in the first, second, and third reproductive seasons. Mutational load was calculated for each population as the difference in mean performance of between-population minus within-population crosses, divided by the mean performance of within-population crosses.

We used data from the same experiment to estimate population growth rates for the 18 populations by constructing and analyzing age-based matrix population models (i.e., Leslie matrices; Caswell 2001). The aim was to determine whether the genomic estimates of load were related to population growth rate in a common environment. The common garden experiment was monitored for 8 years, from 2009 until spring 2016, at which point only four plants remained alive. Survival was tallied each year in early spring. Fecundity was calculated as (flowers + fruits) × (seeds per fruit) × (prob. of germination and seedling survival). Flowers were combined with fruits because in some years the fecundity survey was performed before all fruits had been produced. Over 21,000 fruits were produced across all years, so we did not count seeds in each fruit. Instead, we used the number of seeds per fruit produced in the crossing experiment. These values averaged 17.25 (range 11.56–28.62 across populations) for within-population crosses and 18.46 (12.36–25.91) for between-population crosses. The probability of germination and seedling survival is not known, so we assigned to all populations the value that yielded an average finite rate of increase (λ) of 1 across all populations produced by the within-population crosses. This value was 0.002179, but the results were not qualitatively different if we used a value 10-fold larger or smaller. Estimated Leslie matrices for the populations of plants created by the within-population crosses are in supplementary table S3, Supplementary Material online. For each population we calculated λ, which is the real part of the first eigenvalue obtained by spectral decomposition of the Leslie matrix (Caswell 2001).

Statistical Analysis

Statistical analysis tested whether genomic diversity and genomic estimates of load were associated with the ancestral cluster that populations belonged to (east or west), the distance of the population from the cluster core, and the mating system (outcrossing or selfing/mixed mating). Population outcrossing rates were assessed previously for 18 populations using a progeny-array study in which microsatellite genotypes of maternal plants were compared with their field-produced and lab-reared offspring (Willi and Määttänen 2010, 2011). That analysis showed that outcrossing rate and microsatellite-based inbreeding index of field-collected plants (F_{IS}) are highly correlated and that F_{IS} is a robust indicator of the mating system ($N = 18$, $R^2 = 0.929$, $P < 0.001$). Thus, we deduced the mating system for the remaining populations from their F_{IS} values (Griffin and Willi 2014). Two populations, OE3 and OE1, were not included in Griffin and Willi (2014), so we generated new microsatellite data for them (supplementary table S2, Supplementary Material online).

General linear models were implemented in SAS (SAS Institute Inc. 2013), and data management was executed and figures produced with R (R Core Team 2015). The linear model had the dependent variables of genomic diversity or mutational load and the independent variables of ancestral cluster (east or west), distance to core in km ($\log_{10}$-transformed), and mating system (outcrossing or selfing). Residuals of the dependent variables were graphically investigated for deviations from normality using the kernel density function and qq-plots, and were judged close to normal. The following R packages were used (all last accessed in summber 2016): data.table (Dowle et al. 2015)—for data management; cwhmisc (Hoffmann 2015)—for calculating weighted medians; and adehabitatHR (Calenge 2006), akima (Akima et al. 2015), car (Fox 2016), gdalUtils (Greenberg and Mattiuzzi 2015), GISTools (Brunsdon and Chen 2014), grDevices (R Core Team 2015), mapdata (Becker, Wilks, and Brownrigg 2016), maps (Becker, Wilks, et al. 2015), maptools (Bivand, Lewin-Koh, et al. 2016), PBSmapping (Schnute 2015), RColorBrewer (Neuwirth 2014), rgdal (Bivand, Keitt, et al. 2015), rgeos (Bivand et al. 2016), and sp (Pebesma and Bivand 2005)—for the production of figures. R functions

were downloaded in summer 2016 from: http://www.r-bloggers.com/great-circle-distance-calculations-in-r/—for the calculation of geodesic distances, and http://menugget.blogspot.de/2011/08/adding-scale-to-image-plot.html—for producing color scales. Data files for mapping came from: http://www.naturalearthdata.com/downloads/10m-physical-vectors/ne_10m_lakes/—for lakes, http://gadm.org/- for country, state, and province boundaries, http://geogratis.gc.ca/api/en/nrcan-rncan/ess-sst/a384bada-a787-5b49-9799-f5d589e97bd3.html—for ice sheet extent.

Supplementary Material

Supplementary data are available at *Molecular Biology and Evolution* online.

Acknowledgments

This work was supported by the Swiss National Science Foundation (PP00P3_123396, PP00P3_146342, 31003 A_140979, 31003 A_166322); and the Fondation Pierre Mercier pour la Science, Lausanne. Sequencing was done at the Genetic Diversity Centre ETH Zürich, and at the Department of Biosystems Science and Engineering of ETH Zürich in Basel and the University of Basel. Olivier Bachmann prepared most of the libraries for sequencing. Luca Ferretti, Robert Kofler, and Julie Lee-Yaw gave advice on bioinformatics pipelines and data analysis. We thank Daniel Berner, Ary A. Hoffmann, and Walter Salzburger for helpful comments on the manuscript.

References

Akima H, Gebhardt A. 2015. akima: interpolation of irregularly and regularly spaced data. R package version 0.5-12. https://CRAN.R-project.org/package=akima.

Becker RA, Wilks AR, Brownrigg R. 2016. mapdata: extra map databases. R package version 2.2-6. https://CRAN.R-project.org/package=mapdata.

Becker RA, Wilks AR, Brownrigg R, Minka TP, Deckmyn A. 2015. maps: draw geographical maps. R package version 3.0.1. https://CRAN.R-project.org/package=maps.

Bivand R, Keitt T, Rowlingson B. 2015. rgdal: bindings for the geospatial data abstraction library. R package version 1.1-3. https://CRAN.R-project.org/package=rgdal.

Bivand R, Lewin-Koh N. 2016. maptools: tools for reading and handling spatial objects. R package version 0.8-39. https://CRAN.R-project.org/package=maptools.

Bivand R, Rundel C. 2016. rgeos: interface to geometry engine - open source (geos). R package version 0.3-17. https://CRAN.R-project.org/package=rgeos.

Bridle JR, Vines TH. 2007. Limits to evolution at range margins: when and why does adaptation fail? *Trends Ecol Evol*. 22(3):140–147.

Brown JH. 1984. On the relationship between abundance and distribution of species. *Am Nat*. 124(2):255–279.

Brunsdon C, Chen H. 2014. GISTools: some further GIS capabilities for R. R package version 0.7-4. https://CRAN.R-project.org/package=GISTools.

Calenge C. 2006. The package adehabitat for the R software: a tool for the analysis of space and habitat use by animals. *Ecol Model* 197(3–4):516–519.

Caswell H. 2001. Matrix population models. 2nd ed. Sunderland (MA): Sinauer Associates.

Charlesworth D, Willis JH. 2009. Fundamental concepts in genetics. The genetics of inbreeding depression. *Nat Rev Genet*. 10(11):783–796.

Cingolani P, Platts A, Lily Wang L, Coon M, Nguyen T, Wang L, Land SJ, Ruden DM, Lu X. 2012. A program for annotating and predicting the effects of single nucleotide polymorphisms, SnpEff: sNPs in the genome of *Drosophila melanogaster* strain w^{1118}; *iso*-2; *iso*-3. *Fly* 6(2):80–92.

Dowle M, Srinivasan A, Short T, Lianoglou S, Saporta R, Antonyan E. 2015. data.table: extension of data.frame. R package version 1.9.6. https://CRAN.R-project.org/package=data.table.

Dubchak I, Poliakov A, Kislyuk A, Brudno M. 2009. Multiple whole-genome alignments without a reference organism. *Genome Res*. 19(4):682–689.

Eckert CG, Samis KE, Lougheed SC. 2008. Genetic variation across species' geographical ranges: the central–marginal hypothesis and beyond. *Mol Ecol*. 17(5):1170–1188.

Excoffier L, Foll M, Petit RJ. 2009. Genetic consequences of range expansions. *Ann Rev Ecol Evol Syst*. 40(1):481–501.

Ferretti L, Ramos-Onsins SE, Pérez-Enciso M. 2013. Population genomics from pool sequencing. *Mol Ecol*. 22(22):5561–5576.

Fischer M, Rellstab C, Tedder A, Zoller S, Gugerli F, Shimizu KK, Holderegger R, Widmer A. 2013. Population genomic footprints of selection and associations with climate in natural populations of *Arabidopsis halleri* from the Alps. *Mol Ecol*. 22(22):5594–5607.

Fox J, Weisberg S. 2011. An {R} companion to applied regression. 2nd ed. Thousand Oaks (CA): Sage.

Foxe JP, Stift M, Tedder A, Haudry A, Wright SI, Mable BK. 2010. Reconstructing origins of loss of self-incompatibility and selfing in North American *Arabidopsis lyrata*: a population genetic context. *Evolution* 64(12):3495–3510.

Fracassetti M, Griffin PC, Willi Y. 2015. Validation of pooled whole-genome re-sequencing in *Arabidopsis lyrata*. *PLoS One* 10(10):e0140462.

Gaston KJ. 2009. Geographic range limits: achieving synthesis. *Proc R Soc B* 276(1661):1395–1406.

Gilbert KJ, Sharp NP, Angert AL, Conte GL, Draghi JA, Guillaume F, Hargreaves AL, Matthey-Doret R, Whitlock MC. 2017. Local adaptation interacts with expansion load during range expansion: maladaptation reduced expansion load. *Am Nat*. 189(4):368–380.

Glémin S. 2003. How are deleterious mutations purged? Drift versus nonrandom mating. *Evolution* 57(12):2678–2687.

Greenberg JA, Mattiuzzi M. 2015. gdalUtils: wrappers for the geospatial data abstraction library (gdal) utilities. R package version 2.0.1.7. https://CRAN.R-project.org/package=gdalUtils.

Griffin PC, Willi Y. 2014. Evolutionary shifts to self-fertilisation restricted to geographic range margins in North American *Arabidopsis lyrata*. *Ecol Lett*. 17(4):484–490.

Haldane JBS. 1957. The cost of natural selection. *J Genet*. 55(3):511–524.

Hampe A, Petit RJ. 2005. Conserving biodiversity under climate change: the rear edge matters. *Ecol Lett*. 8(5):461–467.

Hengeveld R, Haeck J. 1982. The distribution of abundance. I. Measurements. *J Biogeogr*. 9(4):303–316.

Henn BM, Botigué LR, Peischl S, Dupanloup I, Lipatov M, Maples BK, Martin AR, Musharoff S, Cann H, Snyder MP. 2016. Distance from sub-Saharan Africa predicts mutational load in diverse human genomes. *Proc Natl Acad Sci U S A*. 113(4):E440–E449.

Henry RC, Barto KA, Travis JMJ. 2015. Mutation accumulation and the formation of range limits. *Biol Lett*. 11(1):20140871.

Hewitt G. 2000. The genetic legacy of the Quaternary ice ages. *Nature* 405(6789):907–913.

Hoffmann CW. 2015. cwhmisc: miscellaneous functions for math, plotting, printing, statistics, strings, and tools. R package version 6.0. https://CRAN.R-project.org/package=cwhmisc.

Hu TT, Pattyn P, Bakker EG, Cao J, Cheng J-F, Clark RM, Fahlgren N, Fawcett JA, Grimwood J, Gundlach H, et al. 2011. The *Arabidopsis lyrata* genome sequence and the basis of rapid genome size change. *Nat Genet*. 43(5):476–481.

Hudson RR. 2002. Generating samples under a Wright-Fisher neutral model of genetic variation. *Bioinformatics* 18(2):337–338.

Hutchinson GE. 1957. Concluding remarks. *Cold Spring Harb Symp Quant Biol*. 22(0):415–427.

Kawecki TJ. 2008. Adaptation to marginal habitats. *Ann Rev Ecol Evol Syst*. 39(1):321–342.
Kimura M. 1955. Solution of a process of random genetic drift with a continuous model. *Proc Natl Acad Sci U S A*. 41(3):144–150.
Kimura M. 1957. Some problems of stochastic processes in genetics. *Ann Math Stat*. 28(4):882–901.
Koboldt DC, Chen K, Wylie T, Larson DE, McLellan MD, Mardis ER, Weinstock GM, Wilson RK, Ding L. 2009. VarScan: variant detection in massively parallel sequencing of individual and pooled samples. *Bioinformatics* 25(17):2283–2285.
Kofler R, Orozco-terWengel P, De Maio N, Pandey RV, Nolte V, Futschik A, Kosiol C, Schlötterer C, Kayser M. 2011. PoPoolation: a toolbox for population genetic analysis of next generation sequencing data from pooled individuals. *PLoS One* 6(1):e15925.
Lande R. 1988. Genetics and demography in biological conservation. *Science* 241(4872):1455–1460.
Lee-Yaw JA, Fracassetti M, Willi Y. 2017. Environmental marginality and geographic range limits in *Arabidopsis lyrata* spp. *lyrata*. *Ecography* 40, 10.1111/ecog.02869.
Li H, Durbin R. 2009. Fast and accurate short read alignment with Burrows-Wheeler Transform. *Bioinformatics* 25(14):1754–1760.
Li H, Handsaker B, Wysoker A, Fennell T, Ruan J, Homer N, Marth G, Abecasis G, Durbin R, 1000 Genome Project Data Processing Subgroup 2009. The Sequence Alignment/Map format and SAMtools. *Bioinformatics* 25(16):2078–2079.
Lohmueller KE, Indap AR, Schmidt S, Boyko AR, Hernandez RD, Hubisz MJ, Sninsky JJ, White TJ, Sunyaev SR, Nielsen R, et al. 2008. Proportionally more deleterious genetic variation in European than in African populations. *Nature* 451(7181):994–998.
Lynch M, Conery J, Bürger R. 1995. Mutation accumulation and the extinction of small populations. *Am Nat*. 146(4):489–518.
Neuwirth E. 2014. RColorBrewer: ColorBrewer palettes. R package version 1.1-2. https://CRAN.R-project.org/package=RColorBrewer.
Ohta T, Cockerham CC. 1974. Detrimental genes with partial selfing and effects on a neutral locus. *Genet Res*. 23(2):191–200.
Paradis E, Claude J, Strimmer K. 2004. APE: analyses of phylogenetics and evolution in R language. *Bioinformatics* 20(2):289–290.
Pebesma EJ, Bivand RS. 2005. Classes and methods for spatial data in R. *R News* 5:9–13.
Peischl S, Excoffier L. 2015. Expansion load: recessive mutations and the role of standing genetic variation. *Mol Ecol*. 24(9):2084–2094.
Peischl S, Kirkpatrick M, Excoffier L. 2015. Expansion load and the evolutionary dynamics of a species range. *Am Nat*. 185(4):E81–E93.
Pickrell JK, Pritchard JK. 2012. Inference of population splits and mixtures from genome-wide allele frequency data. *PLoS Genet*. 8(11):e1002967.
Pollak E. 1987. On the theory of partially inbreeding finite populations. I. Partial selfing. *Genetics* 117(2):353–360.
Press WH, Flannery BP, Teukolsky SA, Vetterling WT. 1992 Numerical recipes in Pascal: the art of scientific computing. Cambridge (United Kingdom): Cambridge University Press.
R Core Team 2015. R: a language and environment for statistical computing. R Foundation for Statistical Computing, Vienna, Austria. https://www.R-project.org/.
Rawat V, Abdelsamad A, Pietzenuk B, Seymour DK, Koenig D, Weigel D, Pecinka A, Schneeberger K. 2015. Improving the annotation of *Arabidopsis lyrata* using RNA-seq data. *PloS One* 10(9):e0137391.
Revell LJ. 2012. phytools: an R package for phylogenetic comparative biology and other things. *Methods Ecol Evol*. 3(2):217–223.
Ross-Ibarra J, Wright SI, Foxe JP, Kawabe A, DeRose-Wilson L, Gos G, Charlesworth D, Gaut BS. 2008. Patterns of polymorphism and demographic history in natural populations of *Arabidopsis lyrata*. *PLoS One* 3(6):e2411.
Roux C, Castric V, Pauwels M, Wright SI, Saumitou-Laprade P, Vekemans X, Ingvarsson PK. 2011. Does speciation between *Arabidopsis halleri* and *Arabidopsis lyrata* coincide with major changes in a molecular target of adaptation? *PLoS One* 6(11):e26872.
Sagarin RD, Gaines SD. 2002. The 'abundant centre' distribution: to what extent is it a biogeographical rule? *Ecol Lett*. 5(1):137–147.
SAS Institute Inc. 2013. SAS 9.4. Cary (NC): SAS Institute.
Schnute JT, Boers N, Haigh R. 2015. PBSmapping: mapping fisheries data and spatial analysis tools. R package version 2.69.76. https://CRAN.R-project.org/package=PBSmapping.
Sexton JP, McIntyre PJ, Angert AL, Rice KJ. 2009. Evolution and ecology of species range limits. *Ann Rev Ecol Evol Syst*. 40(1):415–436.
Sidlauskas B. 2008. Continuous and arrested morphological diversification in sister clades of characiform fishes: a phylomorphospace approach. *Evolution* 62(12):3135–3156.
Simons YB, Turchin MC, Pritchard JK, Sella G. 2014. The deleterious mutation load is insensitive to recent population history. *Nat Genet*. 46(3):220–224.
Smit AFA, Hubley R, Green P. 2015. RepeatMasker Open-4.0. http://www.repeatmasker.org, last accessed summer 2016.
Stoletzki N, Eyre-Walker A. 2011. Estimation of the neutrality index. *Mol Biol Evol*. 28(1):63–70.
Tajima F. 1983. Evolutionary relationship of DNA sequences in finite populations. *Genetics* 105(2):437–460.
Tajima F. 1989. Statistical method for testing the neutral mutation hypothesis by DNA polymorphism. *Genetics* 123(3):585–595.
Vaser R, Adusumalli S, Leng SN, Sikic M, Ng PC. 2016. SIFT missense predictions for genomes. *Nat Protoc*. 11(1):1–9.
Watterson GA. 1975. On the number of segregating sites in genetical models without recombination. *Theor Pop Biol*. 7(2):256–276.
Willi Y. 2013. Mutational meltdown in selfing *Arabidopsis lyrata*. *Evolution* 67(3):806–815.
Willi Y, Määttänen K. 2010. Evolutionary dynamics of mating system shifts in *Arabidopsis lyrata*. *J Evol Biol*. 23(10):2123–2131.
Willi Y, Määttänen K. 2011. The relative importance of factors determining genetic drift: mating system, spatial genetic structure, habitat and census size in *Arabidopsis lyrata*. *New Phytol*. 189(4):1200–1209.
Wright S. 1931. Evolution in Mendelian populations. *Genetics* 16(2):97–159.
Zeng K, Yun-Xin F, Shi S, Wu CI. 2006. Statistical tests for detecting positive selection by utilizing high-frequency variants. *Genetics* 174(3):1431–1439.